

VERY SMALL, ULTRA-WIDEBAND MMIC MAGIC-T AND APPLICATIONS TO COMBINERS AND DIVIDERS

Tsuneo TOKUMITSU, Shinji HARA and Masayoshi AIKAWA*

ATR Optical and Radio Communications Research Laboratories
Radio Systems Department
Sanpeidani, Inuidani, Seika-cho, Soraku-gun, Kyoto 619-02, JAPAN

ABSTRACT

An FET-size, 1-18GHz MMIC magic-T (180° hybrid) which unifies two different dividers, electrically isolated from each other, in a novel GaAs FET electrode configuration based on the "LUFET" concept is proposed. Applications of this module to miniaturized RF signal processing modules such as dividers, combiners, and switches are also described.

INTRODUCTION

Combiners, dividers, and magic-Ts traditionally constructed with quarter-wavelength transmission lines occupy large areas in MMIC chips, and the band widths are limited due to the electrical line lengths[1]. Recently, traveling wave active combiners and dividers which employ GaAs FETs for compact size and wideband operation were reported[2,3]. However, the circuit configuration is still large as well as extremely complicated because several GaAs FETs and many spiral inductors are packed on a chip.

In this paper, a very simple, monolithic active magic-T composed of a two-gate GaAs FET and coplanar lines is proposed. The most significant innovation of the magic-T is a novel circuit structure which effectively uses a two-gate GaAs FET to unify two different dividers within the electrode configuration. This magic-T is based on the "Line Unified FET" (LUFET) concept which was previously proposed by the authors for FET-size, wideband circuit function modules[4]. An advantage of the proposed magic-T is that it remarkably reduces MMIC chip size, as well as operates in an ultra-wideband, due to the minimum use of GaAs FETs and the absence of spiral inductors. Such a miniaturized and wideband magic-T allows applications to many MMICs for RF signal processing.

MAGIC-T CONFIGURATION

The schematic and equivalent circuit of the proposed magic-T is shown in Fig. 1. The active magic-T is composed of a two-gate GaAs FET and coplanar transmission lines unified within the electrode allocation of drain-gate-source-gate-drain. An in-phase power divider, with the coplanar waveguide input port (1) and slotline output ports (1) and (2)

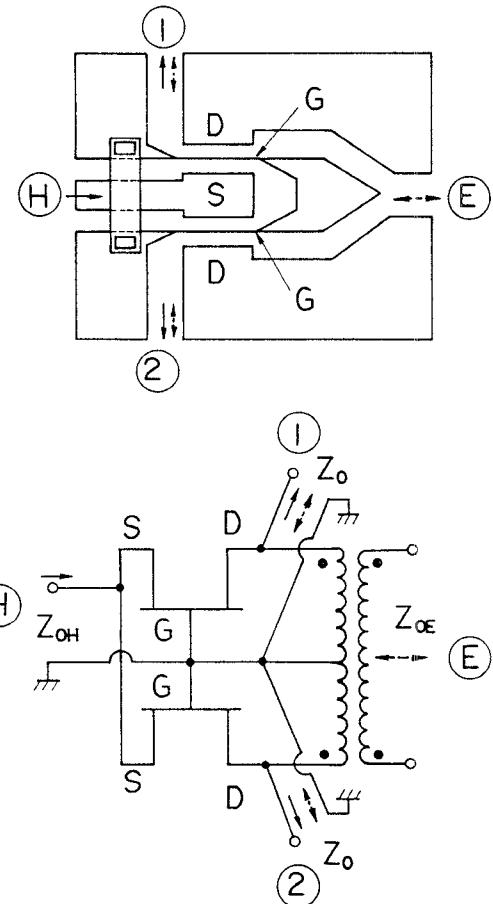
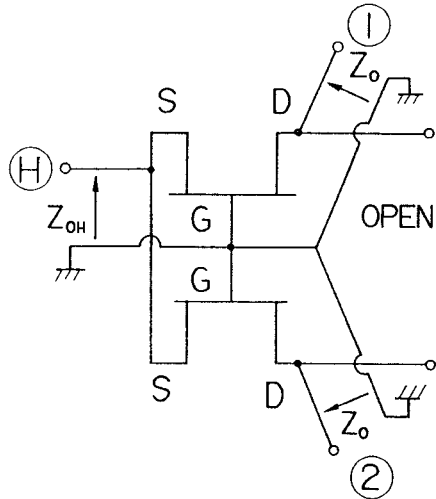


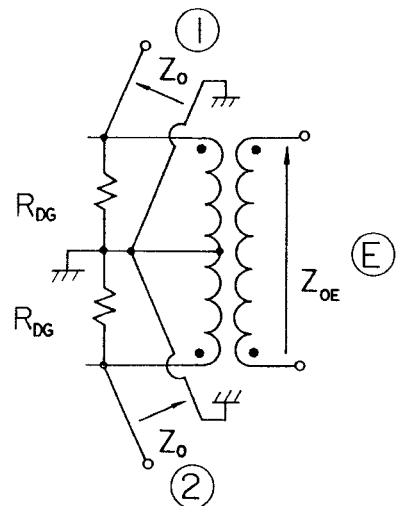
Fig. 1. Configuration and Equivalent Circuit Diagram of the Magic-T

electrically isolated from one another, is realized by the electrode allocation, where the gates serve as the module's common electrode. Furthermore, a slotline series T-junction as an out-of-phase power divider, with the slotline input port (1) and the slotline output ports (1) and (2), is formed with a conductive pad connecting the two gate electrodes and two drain electrodes, one on each side of the pad. In other words,

*M. Aikawa is now with the NTT Radio Communication Systems Laboratories.



(a) In-Phase Power Divider



(b) Out-of-Phase Power Divider

Fig.2. Two Dividers Unified in the Magic-T Configuration

two different dividers are unified in the GaAs FET electrode allocation, while the two dividers are isolated from each other because of the orthogonal mode effect and the unilateral effect of the GaAs FET. The impedance match at port '1' is determined by the transconductance of the two-gate GaAs FET. The impedance at the other ports and the isolation characteristics between ports '1' and '2' are determined by the slotline T-junction and the equivalent resistance between the drain and the gate of each GaAs FET.

MAGIC-T DESIGN

This magic-T operates in an ultra-wideband frequency range because the parasitics in the GaAs FETs are terminated with low impedance Z_0 and because of the absence of frequency-dependent circuitry such as quarter-wavelength transmission lines and spiral inductors. The two dividers, the in-phase power divider and the out-of-phase power divider, are separated as shown in Fig. 2. R_{DG} is the equivalent resistance observed or connected between the drain and the gate of each GaAs FET. The in-phase power divider analysis gives the reflection coefficient $S_{11,11}$ at port (1) and power coupling $|S_{12,11}|$, $|S_{21,11}|$ from port (1) to ports (1) and (2) as shown in equation (1) and (2).

$$S_{\oplus\oplus} = \frac{1-2g_m Z_{OH}}{1+2g_m Z_{OH}} \quad (1)$$

$$|S_{\oplus\oplus}| = |S_{\ominus\oplus}| = \frac{2g_m\sqrt{Z_{OH}Z_0}}{1+2g_mZ_{OH}} \cdot \frac{R_{DG}}{R_{DG}+Z_0} \quad (2)$$

where, g_m is the transconductance of each common-gate GaAs FET. The isolation from ports (1) and (2) to port (H) is due to the unilateral characteristic of each

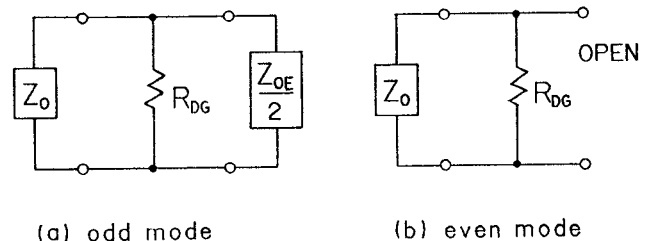


Fig. 3. Orthogonal Mode Analysis of the Out-of-Phase Power Divider

GaAs FET. The reflection coefficient $|S_{11}^{(1,2)}|$ is at its minimum, that is zero, when $2gmZ_0=1$, while the power coupling $|S_{12}^{(1,2)}|$, $|S_{21}^{(1,2)}|$ is about -6dB . The out-of-phase divider analysis, as shown in Fig. 3, through an orthogonal mode analysis based on the symmetrical configuration of the slotline series T-junction yields the following equations giving the reflection coefficient $|S_{11}^{(1,2)}|$, $|S_{22}^{(1,2)}|$, $|S_{12}^{(1,2)}|$ at ports (1), (2) and (3), the isolation $|S_{121}^{(1,2)}|$, $|S_{212}^{(1,2)}|$ between ports (1) and (2), and the power coupling $|S_{112}^{(1,2)}|$, $|S_{221}^{(1,2)}|$, $|S_{122}^{(1,2)}|$, $|S_{211}^{(1,2)}|$ between ports (1) or (2) and port (3).

$$|S_{\oplus\oplus}| = |S_{\ominus\ominus}| = \frac{|\Gamma_{+-} + \Gamma_{++}|}{2} \quad (3)$$

$$|S_{\textcircled{1}\textcircled{2}}| = |S_{\textcircled{2}\textcircled{1}}| = \frac{|\Gamma_{+-} - \Gamma_{++}|}{2} \quad (4)$$

$$|S_{\oplus\ominus}| = |\Gamma_{+-}| \quad (5)$$

$$|S_{\textcircled{2}\textcircled{1}}| = |S_{\textcircled{2}\textcircled{2}}| = |S_{\textcircled{1}\textcircled{2}}| = |S_{\textcircled{1}\textcircled{2}}|$$

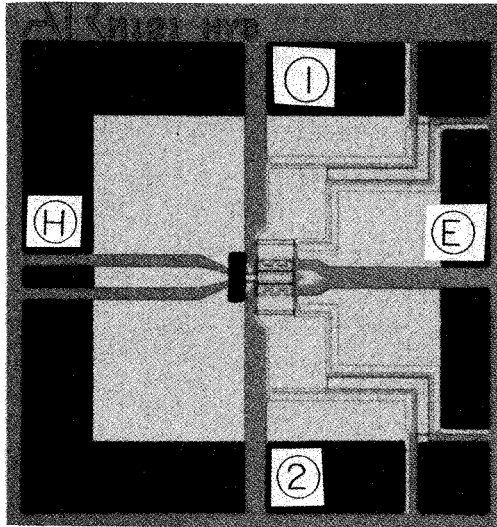


Fig.4. Photograph of the Magic-T on a 1×1mm Chip

$$= \sqrt{\frac{1-|\Gamma_{+-}|^2}{2}} \cdot \frac{2R_{DG}}{2R_{DG}+Z_0} \quad (6)$$

where, the reflection coefficient Γ_{+-} , Γ_{++} at port (1) in each excitation mode is given by following equations.

$$\text{Odd: } \Gamma_{+-} = \frac{(Z_{OE} \parallel 2R_{DG}) - 2Z_0}{(Z_{OE} \parallel 2R_{DG}) + 2Z_0}, \text{ Even: } \Gamma_{++} = \frac{R_{DG} - Z_0}{R_{DG} + Z_0}$$

The power coupling given by equation (6) is less than -3.5dB . The difference between the coupling given by equation (2) and (6) can be less than 2dB when $2gmZ_0$ is greater than 1.2. The resistor R_{DG} acts to reduce the reflection coefficient at ports (1) and (2), and to increase the isolation between ports (1) and (2).

EXPERIMENT RESULTS

A photograph and the performance of the fabricated magic-T are shown in Fig. 4 and Fig. 5, respectively. The chip size is $1\text{mm} \times 1\text{mm}$ (the intrinsic area is only $150\mu\text{m} \times 250\mu\text{m}$).

The ultra-wideband characteristics of the magic-T have been confirmed through on-wafer measurements up to 18 GHz as shown in Fig. 5 : coupling loss from port (1) or (2) to port (1) and (2) is within $5\text{dB} \pm 1\text{dB}$; return loss at each port is greater than 10 dB ; isolation is greater than 20 dB except between ports (1) and (2), which is about 10 dB . Phase difference between outputs of the out-of-phase divider is within $180^\circ \pm 10^\circ$. The reason the measured isolation between ports (1) and (2) is better than predicted, is believed to be due to the module's configuration. A spatial coupling, for example, between the coplanar waveguide and the slotlines separated by the gate electrodes, improves Γ_{++} improving the isolation. The equivalent resistance R_{DG} in each excitation mode should be estimated individually for more accurate design.

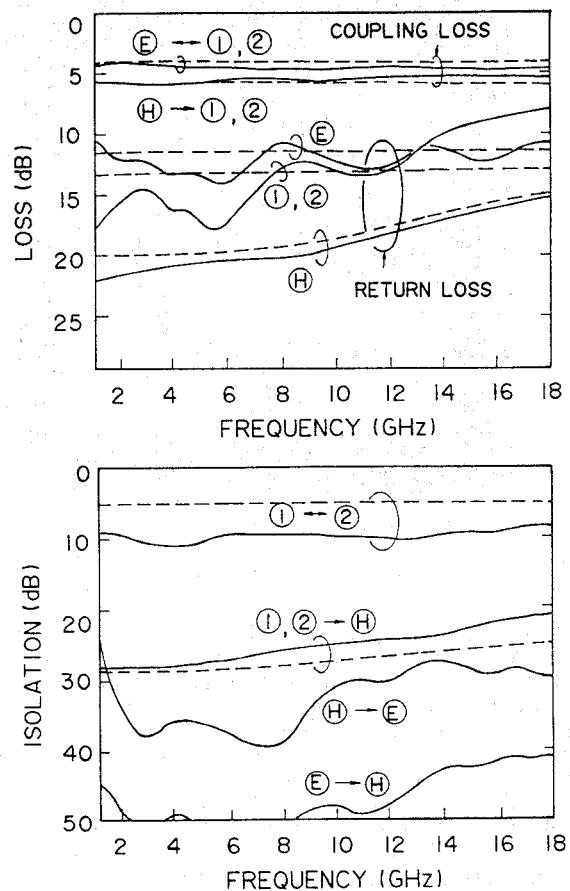
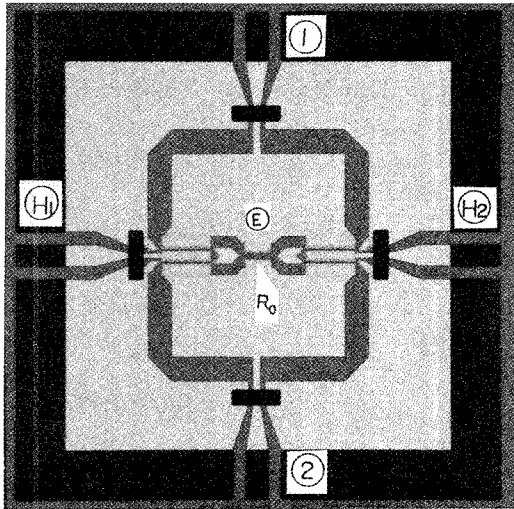


Fig. 5. Performance of the Magic-T (Solid Line : Measured, Dashed line : Predicted)

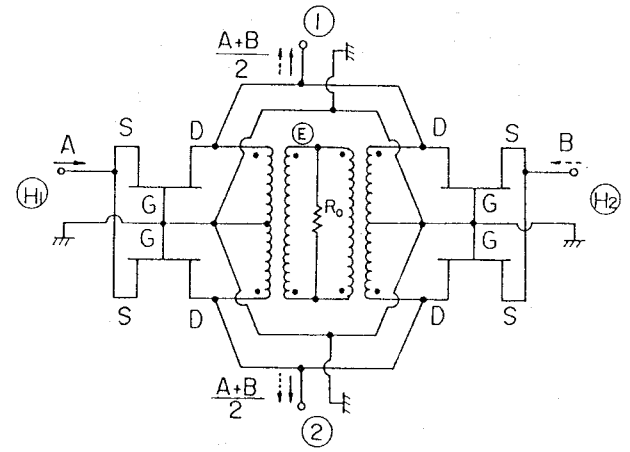
APPLICATION TO A SIGNAL DIVIDER/COMBINER

A photograph and the equivalent circuit diagram of a signal divider/combiner utilizing the proposed magic-T is shown in Fig. 6. Two magic-Ts are combined symmetrically at ports (1), (2) and port (4) where a shunt resistor R_0 is connected. The characteristics of the signal divider/combiner and the magic-T are represented in a similar fashion because the only changes in the above equations are R_{DG} to $R_{DG}/2$ and Z_{OE} to R_0 . Therefore, signal power division from port (H) or (H₂) to ports (1) and (2) is achieved maintaining port isolation in the magic-T. Isolation between output ports (1) and (2) is significantly improved by increasing R_0 value. Figure 7 shows the performance of the fabricated divider / combiner shown in Fig. 6, where R_0 is given two different values, 50Ω and infinite. Coupling loss from port (H) or (H₂) to ports (1) and (2) is almost the same for both R_0 values, while isolation between ports (1) and (2) is changed considerably by the R_0 value.

Advantages of this divider / combiner are that it operates in an ultra-wideband frequency range, as well as offers the following useful functions in small MMIC chip size. This module divides RF incident signals, A



(a) Photograph (Chip Size : 1mm \times 1mm)



(b) Equivalent Circuit Diagram

Fig.6. Configuration and Equivalent Circuit Diagram of the Signal Divider/Combiner.

and B on port H_1 and H_2 respectively, and simultaneously generates the same combined signals $(A+B)/2$ at ports ① and ② with good isolation. This module can also be used to change the signal path with H_1-H_2 isolation better than 25dB by controlling the gate-source voltages for the two GaAs FETs. It can also switch the signal flow between ports ① and ② by controlling the value of R_0 . These functions are not possible with passive circuits. An adaptive linear combiner as the basic form of adaptive equalizer, and switch matrixes are the examples where effective divider/combiner module use. As a result, this module can be used as one of the fundamental function blocks for RF signal processing such as array antenna controls and multi-port RF switching.

CONCLUSION

A very small, ultra-wideband MMIC magic-T and a signal divider/ combiner using a magic-T are proposed. These modules can be efficiently used for microwave and millimeter-wave MMICs such as mixers and many types of RF processing.

ACKNOWLEDGMENTS

The authors would like to thank Dr. Kohei Habara, vice president of Advanced Telecommunications Research (ATR) Institute International, and Dr. Yoji Furuhama, president of ATR Optical and Radio Communications Research Laboratories, for their helpful discussions and valuable suggestions.

REFERENCES

[1] G. K. Lewis, et al. "GaAs MMICs FOR DIGITAL RADIO FREQUENCY MEMORY (DRFM) SUB-SYSTEMS," IEEE Microwave and Millimeter-wave Monolithic Circuits Symposium Digest, pp. 53-56, 1987

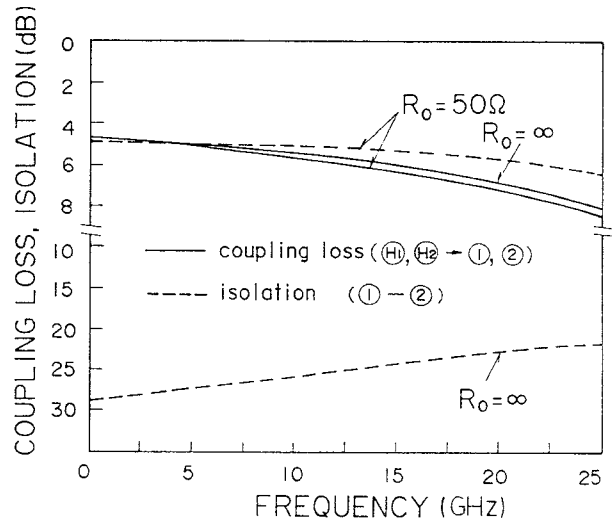


Fig. 7. Performance of the Fabricated Divider/Combiner.

[2] G. S. Barta, et al. "A 2 to 8GHz LEVELING LOOP USING A GaAs MMIC ACTIVE SPLITTER AND ATTENUATOR," IEEE Microwave and Millimeter-wave Monolithic Circuits Symposium Digest, pp. 75-79, 1986

[3] D. Levy, et al. "A 2-18GHz MONOLITHIC PHASE SHIFTER FOR ELECTRONIC WARFARE PHASED ARRAY APPLICATIONS," IEEE GaAs IC Symposium Digest, pp. 265-268, 1988

[4] T. Tokumitsu, et al. "ACTIVE ISOLATOR, COMBINER, DIVIDER, AND MAGIC-T AS MINIATURIZED FUNCTION BLOCKS," IEEE GaAs IC Symposium Digest, pp. 273-276, 1988